Degradation of Bisphenol a Using Horseradish Peroxidase Immobilized on Fe-based MOFs

Wenting Cai
South China University of Technology
Jiaxin Xu
South China University of Technology
Jianhua Cheng (jhcheng@scut.edu.cn)
South China University of Technology
Kesi Du
South China University of Technology
Yuancai Chen
South China University of Technology

Research Article

Keywords: MIL-88B (Fe), Immobilized enzyme, Covalent fixation, Horseradish peroxidase, Bisphenol A, Degradation

Posted Date: February 9th, 2021

DOI: https://doi.org/10.21203/rs.3.rs-166722/v1

Abstract

In this study, we synthesized a water-stable Fe-based metal-organic framework, MIL-88B (Fe) by a solvothermal method, and for the first time, MIL-88B (Fe)/HRP composite was prepared for the degradation of bisphenol A (BPA) by immobilizing horseradish peroxidase on MIL-88B (Fe) using covalent fixation method. The material was characterized via XRD, FTIR, TG, and SEM methods. The results showed that the composite could remove bisphenol A quickly and efficiently by adding the hydrophilic agent polyethylene glycol, with the removal rate of BPA up to 99.2% within 1 hour. In addition, the initial concentration of bisphenol A, the dosage of the immobilized enzyme and the amount of H_2O_2 added had a great influence on the degradation efficiency. It was found that immobilized HRP could be reused, and its storage stability and thermal stability were better than free HRP. These show that immobilized enzymes have a broad application prospect in waste-water treatment.

Highlights

1. Horseradish peroxidase is immobilized on MIL-88B(Fe) for the first time for waste-water treatment application.
2. Immobilized HRP shows better pH, temperature and storage stability than free HRP.
3. The optimal degradation conditions for the highest removal efficiency are evaluated.
4. 2% of bisphenol A can be degraded within 60 min under the catalyst dosage of 0.10g/L.
5. MIL-88B(Fe)/HRP can be reused after BPA degradation.

Introduction

Bisphenol A (BPA) is a raw material for synthetic plastics, which can be made into a variety of common plastic products, such as water bottles, sports equipment, medical devices and so on. For the unreasonable use, it can be extensively found in industrial waste-water, surface water, groundwater and even drinking water (Luo et al. 2019). BPA has neurotoxicity, immunotoxicity, carcinogenicity and teratogenicity, which can affect the endocrine system of humans and animals, leading to the feminization of male animals and the reduction of reproductive ability (Zhang et al. 2020b). Therefore, the degradation of BPA has a great significance to the ecological environment and human health.

At present, many techniques have been explored for the removal of bisphenol A, including physical, chemical, biological methods, etc. (Bhatnagar &Anastopoulos 2017, Lin et al. 2020, Zhang et al. 2020a). Among them, enzymatic treatment has been widely used due to the high degree of speed and high selectivity (Besharati Vineh et al. 2018). Horseradish peroxidase (HRP) is a heme protein with an iron porphyrin active center, which can oxidize and degrade bisphenol A in the presence of H_2O_2. After oxidized to free radicals, the substrate molecules can be rearranged and coupled to form corresponding polymers and other compounds, which are non-toxic and can be easily removed from water (Pylypchuk et al. 2020). Nevertheless, the free HRP has many drawbacks including poor thermal and storage stability,

high cost for no reusability and recyclability. Thus, researchers have been looking for materials with superior properties to overcome the shortcomings in enzyme applications.

Metal organic frameworks (MOFs) is a crystalline porous material with periodic network structure formed by self-assembly of metal ions and organic ligands through complexation. It has been proved that MOFs can be used for enzyme covalent immobilization. Shih et al. (2012) fixed trypsin (Try) to MIL-88B-NH_2 (Cr) through DCC, and used it for bovine serum protein (BSA) degradation. Doherty et al. (2013) used glutaraldehyde to immobilize β-glucosidase on NH_2-MIL-53(A1) for catalytic hydrolysis of D-salicylic acid into glucose. MIL-88B (Fe) is a water-stable Fe-based MOF with great performance (Laurier et al. 2013). Inspired by previous works, we successfully immobilized horseradish peroxidase on MIL-88B(Fe) for the first time, and explored various influencing factors for the degradation of BPA by immobilized enzyme. The results showed that Fe-MOF had obvious advantages, with the removal rate of BPA up to 99.2% within 1 hour under the catalyst dosage of 0.10g/L. What's more, after fixation, the storage stability of HRP was improved, which provided the possibility of applying the material to the treatment of BPA in water environment.

Experimental

2.1. Materials

HRP (≥160 units/mg, freeze-dried powder, RZ≥2), bisphenol A (BPA, 99.0%), iron (III) chloride hexahydrate ($FeCl_3 \cdot 6H_2O$, 99%), 1,4-Benzenedicarboxylic (H_2BDC, 99%), N-Hydroxysuccinimide (NHS, 98%), N-(3-Dimethylaminopropyl)-N'-ethylcarbodiimide hydrochloride (EDC, 98.0%), N, N-dimethylformamide (DMF, 99.5%), ethanol (C_2H_5OH, 99.7%) and phenol were purchased from Aladdin Reagent Co., Ltd. (Shanghai, China). 4-aminoantipyrine (4-AAP, 98%), H_2O_2 (30% *m/m*) and polyethylene glycol (PEG) were purchased from Sinopharm Chemical Reagent Co, Ltd. (Shanghai, China). All reagents were analytical grade and used without further purification.

2.2. Characterization

X-ray diffraction (XRD) patterns of MIL-88B(Fe) powder and MIL-88B(Fe)/HRP composite were obtained via using a Bruker D8 Advance X-ray diffractometer. Fourier transform infrared (FTIR) spectra of the products were carried on a Thermo-Nicolet spectrometer (CCR-1; USA). And then, scanning electron microscope (SEM, Carl Zeiss Microscopy, Germany) was employed to observe the morphologies of samples. The thermal stability was measured on a TG-DTG 6300 thermogravimetric analyzer (EXSTAR, Japan) by heating samples to 600℃ at a rate of 5 ℃/min in 60 mL/min air flow.

2.3. Synthesis of MIL-88B(Fe)

MIL-88B(Fe) was prepared by a solvothermal method according to the literature with some key improvement (Yi et al. 2020). $FeCl_3 \cdot 6H_2O$ (756.3 mg, 2.77 mmol), H_2BDC (253.4 mg, 1.385 mmol) and 60mL DMF were mixed and stirred for 30 min to form a homogenous solution. The mixture was

transferred into the Teflon autoclave and placed in the oven at 150 ℃ for 2 hours. When the reaction finished, the product was gathered by centrifugation and washed several times with ethanol and dried under vacuum at 60 ℃ overnight.

2.4. Enzyme immobilization

MIL-88B(Fe) (10 mg), EDC (40mg), NHS (20mg) were dispersed in enzyme solution (0.04mg/ml, 10ml) and stirred with a magnetic stirrer for 8 hours at 30℃. The mixture was gathered by centrifugal collection and rinsed with deionized water several times to remove non-specifically unbound enzyme. The supernatant with residual enzyme was collected to measure the quantity of protein loading with UV/Visible spectroscopy (λ=595nm) using the Bradford method (Wang et al. 2015). The MIL-88B(Fe)/HRP was dispersed in deionized water and stored in refrigerator at 4 °C.

2.5. Assays of enzymatic activity

A colorimetric method was used to determine the activity of the enzyme using phenol, 4-AAP, and H_2O_2 as substrates (Chang &Tang 2014). The catalytic reaction was monitored by recording the absorbance of the red product at 510 nm. One unit of activity was defined as the amount of HRP required to hydrolyze 1 × 10^{-6} mol of H_2O_2 per minute under the conditions stated above.

2.6. Degradation experiments

Degradation experiments were conducted in conical flasks (150 mL) and vigorously stirred with magnetic stirrers. Reagents were added in the following order: bisphenol A (10 –100 mg/L) solution, 2.5 ml phosphate buffer (pH 7, 200 mM), 1mg/ml PEG (0.1– 0.8 ml), H_2O_2 and MIL-88B(Fe)/HRP material (1- 5 mg). At predefined intervals, the supernatant was removed by syringes and filtered through 0.22-μm filters. All experiments were carried out three times and the results were averaged. BPA was detected by high performance liquid chromatography (HPLC, Waters, USA) at the wavelength of 270 nm, which equipped with a photo-diode array (PDA) detector. The mobile phase was methanol/ultrapure solution (70:30, v/v), and the flow was 1.0 mL·min^{-1}. In addition, the injection volume of the samples was 10 μL and the column was operated at 303 K.

2.7. Recycling experiments

After each cycle, the used MIL-88B(Fe)/HRP was separated by centrifugation and washed with deionized water to remove any residual reaction solution within material. After that, the catalyst was reused in a new reaction medium under the experimental conditions described previously. Each round of the degradation was carried out at 25 °C and the retained activity was determined.

Results And Discussion

3.1. Characterization of Materials

Fig. 1(a) showed that the form of MIL-88 (Fe) was a spindle-like material. The existence and uniform distribution of Fe, C and O elements in MIL-88B (Fe) were confirmed by energy dispersion-X ray spectroscopy. Because of the abundant amino groups, HRP could be immobilized on MIL-88 (Fe) using EDC/NHS induced covalent reaction. After immobilization, the morphology of Fe-MOF remained unchanged (Fig. 1b).

The XRD patterns of the as-synthesized MIL-88B(Fe) were shown in Fig. 2a. They matched well with the diffraction peaks of MIL-88B (Fe) [0 0 2], [1 0 1], [1 0 3], [2 0 2] and [2 1 1] as well as the previously reported (Lei et al. 2018). The high intensity diffraction peaks proved the successful synthesis of MIL-88 (Fe). Meanwhile, there were no other peaks, indicating that a pure phase MIL-88B(Fe) was obtained. It should be pointed out that due to the flexibility of the MOF material structure, the peak position and strength will vary slightly (Gao et al. 2017). From the XRD patterns of MIL-88B(Fe)/HRP, it could be clearly seen that the five characteristic peaks were the same and the positions were all well matched. The results suggested that the structural integrity and crystalline morphology of MIL-88B(Fe) were preserved in the presence of HRP and the binding process did not lead to the phase change. What's more, the decline in peak intensity indicated that the enzyme was successfully loaded.

In order to further ascertain the molecular structure and functional groups of MIL-88B(Fe), FTIR spectrum was performed. As displayed in Fig. 2(b), the characteristic absorption peaks were the same as those reported in literature (Vu et al. 2017), and were observed at 552, 1394 and 1548 cm^{-1}, respectively. The strong band at 552 cm^{-1} was designated as Fe-O vibrations. The two peaks at 1548 and 1394 cm^{-1} were considered to be asymmetric and symmetric vibrations of the carboxyl group, which confirmed the presence of dicarboxylic acid ligand in MIL-88B (Fe) material (Lin et al. 2020). In the FT-IR curve of MIL-88(Fe)/HRP, the peak of 1029.93 cm^{-1} was attributed to the N-H bending vibration of the amide bond within the protein characteristic structure region of 1174-955 cm^{-1} (Samui &Sahu 2018). The characteristic peak at 3,700 - 3000 cm^{-1} was attributed to -OH and -NH groups (Jia et al. 2019). As expected, the characteristic absorption peaks of MIL-88B(Fe) still emerged in the FT-IR spectrum of immobilized enzyme bio-composite, which marked the successful formation of MIL-88(Fe)/HRP.

The TGA curves showed that MIL-88B (Fe) had good thermal stability. When the temperature was above 350℃, the structure collapsed (rapid weight loss). The TGA curve of MIL-88(Fe)/HRP showed two distinct weightlessness steps (Fig. 2c). The first weight loss was due to evaporation of adsorptive and bound water and enzyme decomposition (Zhang et al. 2020c). The second weight loss was the collapse of the MOF skeleton, which was consistent with the trend of MIL-88B (Fe). When the temperature reached 450℃, the immobilized enzyme retained 29.9% of its initial weight, which was slightly higher than 25.3% of MIL-88B(Fe). This was due to some organic residues left in the pyrolysis process of immobilized HRP (Wu et al. 2019).

3.2. Effect of reaction conditions

3.2.1. Reaction time and effect of PEG

The degradation experiments for BPA (20 mg/L) at pH 7.0 were performed to evaluate the catalytic nature of as-synthesized materials. As shown in Fig. 3a, MIL-88(Fe) exhibited poor adsorption performance, only 22.6% of bisphenol A removal within 3 h. Under the same conditions, almost 50.5% of BPA was removed when MIL-88(Fe)/HRP served as the catalyst in an hour, but then the reaction was terminated because the enzyme was inactivated. It has been reported that the inactivation of horseradish peroxidase is due to the attachment of free radicals and polymeric products to the enzyme in the catalytic cycle (Dalal &Gupta 2007). In order to prevent this, some researchers have suggested that highly hydrophilic additives such as PEG can be added to the reaction system. PEG can form a protective layer in the vicinity of the HRP active center, limiting the free phenoxy radicals formed during the reaction to inactivate enzyme. Also, PEG has a stronger affinity with degradation products than enzyme, which prevents HRP from being absorbed (Cheng et al. 2006). With the aid of PEG, MIL-88(Fe)/HRP materials successfully achieved significant degradation of BPA and showed excellent catalytic properties compared with previous reports (Table 1).

Table 1. The BPA removal rate of enzyme immobilized with different materials.

Immobilized material	Enzyme	$C_{catalysts}$	C_{BPA}	Degradation performance	Ref.
H. communis scaffolds	Laccase	1.00 g/L	2 mg/L	24 h, ≈95 %	(Zdarta et al. 2018)
MCMSs	Laccase	2.00 g/L	20 mg/L	12 h, 85%	(Lin et al. 2016)
PFM	HRP	0.1425 g/L	8.7 mg/L	180 min, 93%	(Xu et al. 2013)
TiO_2 sol–gel coated PVDF membranes	Laccase	≈0.40 g/L	34.5 mg/L	96 h, 91.7%	(Hou et al. 2014b)
NF membranes	HRP	120 U/L	20 mg/L	180 min, 95%	(Escalona et al. 2014)
APTES modified TiO_2	Laccase	500 U/L	34.5 mg/L	5 h, ≈80 %	(Hou et al. 2014a)
magnetic silk fibroin nanoparticles	HRP	500 U/L	50 mg/L	160 min, 80.3%	(Xu et al. 2011)
MCN	HRP	0.5 g/L	10 mg/L	50 min, 85.7%	(Zhang et al. 2020a)
MIL-88(Fe)	**HRP**	**0.10 g/L**	**20 mg/L**	**60 min, 99.2%**	**Present work**

The effect of reaction time: When the catalyst dosage was 0.06g/L and the initial concentration of BPA was 20mg/L, it could be seen that the degradation rate occurred speedily in the initial 60 min, then

slowed down with the increase of time and the degradation equilibrium was basically reached at 3 h with a removal rate of 98.4%. Therefore, the optimal reaction time for the degradation experiments was determined to be 3 h.

The effect of PEG dosage: When the mass ratio of PEG/BPA was 0.1, the degradation rate of BPA was 72.7% (Fig. 3b). With the increased amount of PEG, the removal rate of BPA was significantly increased. This was due to a decrease in the amount of enzymatic inactivation and the degradation reaction was allowed to continue. When the value was 0.4, the degradation rate peaked at 98.4% and remained unchanged for the further addition of PEG. Therefore, subsequent experiments were all carried out in the presence of PEG and the mass ratio of PEG/BPA was equal to 0.4.

3.2.2. pH values

The effect of pH values on BPA degradation with MIL-88(Fe)/HRP was investigated. The consequences are shown in Fig. 4a. When pH ranged from 5 to 7, the removal rate was all at a high level. The optimum pH was observed at pH = 6, with maximum catalytic effect of 98.5% in 3 h. The increased pH had an adverse effect on materials, for the degradation rate slightly decreased when pH was 9. This was caused by the denaturation of enzymes under alkaline conditions. However, there was still above 90% of BPA removed, which demonstrated that the immobilized enzyme could better withstand pH changes. This might be owing to the multi-point covalent bonding on the MIL-88B(Fe) carrier to stabilize the enzyme molecules (Wang et al. 2014).

It is worth noting that at pH =5, the degradation rate of BPA was slightly lower at the beginning, but increased after 40 minutes. This may be due to the leaching of iron ions, resulting in a Fenton reaction in the presence of H_2O_2. It has been reported that at pH =5, the iron leaching rate of MIL-88B(Fe) is 0.5 mg/L at 30 min and the concentration increases with reaction time (Gao et al. 2017). The leached Fe^{3+} was reduced to Fe^{2+} by reducing substances in the system and reacted with H_2O_2, promoting the degradation of BPA.

3.2.3. H2O2 concentration

The co-substrate H_2O_2 can activate the enzymatic reaction, thus the removal percentage is highly dependent on the ratio of H_2O_2 and substrate concentration (Lu et al. 2017). Fig. 4b shows that the highest catalytic efficiency appears at n (H_2O_2): n (BPA) = 1.5:1. When the molar ratio was lower than 1.5, the reaction was inefficient and the amount of BPA removed raised significantly with an increase in hydrogen peroxide concentration, which showed that H_2O_2 was the limiting factor in this range. It could also be seen that the molar ratio of H_2O_2 and BPA ranged from 1.5:1 to 2:1, the removal rate was basically the same, both at the highest value. This is consistent with the results reported in previous literature that the optimal ratio on the treatment of BPA by horseradish peroxidase is 1.5 or greater than 1.5 (Hong-Mei &Nicell 2008, Xiao et al. 2020).

3.2.4. Reaction temperature

The optimum temperature of BPA degradation using synthesized materials was investigated. Fig. 4c showed that the maximum degradation rate for BPA was reached at 25°C. This was due to the high catalytic activity of HRP under this condition. At the temperature of 55°C, it could be seen that the catalyst efficiency of BPA by the immobilized HRP slowed down and the removal rate was at a low level. This was because enzymes were inactivated by prolonged exposure to high temperatures. Therefore, the optimal temperature for the reaction is 25°C.

3.2.5. Bisphenol A concentration

The bisphenol A concentration in the aqueous phase can affect HRP mediated reactions and the results are shown in Fig. 4d. Apparently, MIL-88B(Fe)/HRP exhibited the highest degradation efficiency when the concentration of BPA was 10 mg/L, and the removal efficiency decreased with increasing BPA concentration from 10 to 100 mg/L. The reason might be that the BPA molecules adsorbed on the surface of the material blocked the active site on the HRP, resulting in the reduction of the formation of active substances (Cao et al. 2020). In addition, with the increase of BPA concentration, the enzyme-catalyzed reaction rate tended to be balanced, thus the removal rate of BPA began to slow down. It is noticed that even at a concentration of 100 mg/L, 93.1% of BPA was removed within 4 hours. This shows the excellent degradation performance of MIL-88B(Fe)/HRP and its good prospects in wastewater treatment applications.

3.2.6. Optimum catalyst dose

The effect of catalyst dosages on BPA removal was also studied. As illustrated in Fig. 4e, the degradation efficiency of BPA improved rapidly when the materiel dose increased from 0.02 to 0.10 g/L, which was because of the increase of catalytic activity sites for BPA degradation. At the catalyst dosage of 0.10 g/L, 99.2% of BPA was removed within one hour. The most expensive part of enzymatic treatment of wastewater depends on the enzyme, so the balance between the catalytic efficiency and the cost should be considered. In addition, in order to make the reaction not to proceed too fast and easy to measure, 0.06 g/L is chosen as the optimum catalyst dose for BPA degradation in the experiments.

3.3. Michaelis-Menten kinetics

The kinetic parameters (K_m and V_{max}) of the free and immobilized HRP were calculated by Michaelis-Menten and Lineweaver-Burk plots and the results were shown in Fig. 5. With the increase of substrate concentration, the enzymatic reaction rate first increased and then tended to be stable (Fig. 5a). Compared with free enzyme, immobilized HRP had a lower reaction rate due to the limited mass transfer (Bilal et al. 2020). K_m refers to the affinity between the enzyme and the substrate, and the smaller the K_m value is, the higher the affinity is. The K_m of free HRP was 0.34 mM, while immobilized enzyme increased to 0.47 mM, and the V_{max} decreased from 19.23 mM $\cdot min^{-1}$ to 14.28 mM $\cdot min^{-1}$ (Fig. 5b). This was

because the covalent fixation changed the conformation of enzyme, hindered the contact between the substrate and HRP active site, reduced the affinity and the maximum reaction rate.

3.4. Thermal and storage stability

In industrial applications, the denaturation of enzymes caused by high temperature is also an urgent problem to be solved. Therefore, the thermostability of the immobilized and free HRP was conducted by measuring the residual activity after incubating in the temperature range from 25°C to 60 °C for an hour. It can be seen from Figure 6a that after 60℃ heat treatment, the residual activity of free HRP decreased to 55.9%, while the immobilized HRP still maintained 70.2% of the initial value. What's more, the activity of MIL-88B(Fe)/HRP was higher than that of free enzyme at different temperatures. These results indicate that immobilized enzyme is more heat resistant than free enzyme, which may be due to limited conformational changes of enzyme. The protective effect of MIL-88B(Fe) can constrain the unfolding and nonspecific aggregation of the enzyme molecules and thus prevent thermal denaturation of HRP (Vineh et al. 2020).

The storage stability of synthesized samples is an important index to assess the immobilized efficiency. Both MIL-88B(Fe)/HRP and free HRP were evaluated by measuring the residual activity after 30 days of storage in deionized water at 4°C (Fig. 6b). As expected, the activity of MIL-88B(Fe)/HRP declined much slower than that of free enzyme. The immobilized HRP retained as high as 90% of its initial viability during storage for 15 d, whereas the free HRP decreased to 64% of enzyme activity. After 30 days, only 26.2% initial activity could remain for free HRP, while for the synthesized materials, the activity reached over 70%. The loss of activity of free HRP might be caused by conformational changes during storage, and the active sites could not react with the substrates (Chang et al. 2016). On the contrary, MIL-88B(Fe)/HRP showed great resistance to conformational changes due to the formation of strong covalent bonds with enzyme. This could be further interpreted as the protective effect of samples on the potential adverse warping effect of aqueous solution on HRP active sites (Zhai et al. 2013). Therefore, immobilized enzyme is more stable and has a longer shelf life than free HRP. The result shows that MIL-88B(Fe)/HRP has great durability and shows extraordinary potential in industrial application.

3.4. Reusability of immobilized HRP

One of the main purposes of enzyme immobilization is the performance of its reuse. This is because enzymes are mostly expensive and unstable compared to conventional chemical catalysts. Enzyme immobilization can restore the catalytic samples easily and stabilize the active conformation of the enzyme. The reusability of MIL-88B(Fe)/HRP was studied by assessing the degradation rate of BPA after successive service times. As shown in Fig. 6c, the immobilized HRP can be reused for up to two cycles with little change in its retained activity, which may be connected with the strong covalent bond formed by HRP and MIL-88B(Fe) through EDC/NHS. This may inhibit the shedding of enzyme resulting from repeated washing, thus effectively preventing reduction of activity (Hu et al. 2018). After 5 cycles, the residual activity still retained 55.2%, indicating that the catalytic samples are stable and can be recycled. What's more, the relative activity of synthesized materials is reduced with the increase of reuse times.

There are several possible reasons for this phenomenon. (1) Due to the trace amounts of samples, part of the MIL-88B(Fe)/HRP are lost in the recycling process. (2) The accumulation of the products on the materials during the reaction may hinder the active sites of HRP and have an adverse effect on the next reaction cycle (Chang et al. 2015). (3) Part of HRP is folded or denatured during the reaction with the substrate, resulting in enzyme inactivation (Shakerian et al. 2020). In conclusion, the immobilized enzyme has the advantages of simple separation and good stability, which can greatly reduce the actual application cost of the enzyme system and can be successfully used in continuous preparation.

Conclusion

In summary, we immobilized HRP on MIL-88B(Fe) through EDC/NHS covalent cross-linking system to obtain MIL-88B(Fe)/HRP composite and used it for the degradation of BPA. The results showed that the hydrophilic substance PEG could greatly improve the degradation efficiency, and 99.2% BPA with an initial concentration of 20mg/L could be degraded within 1 hour with the addition of 0.1g/L immobilized enzyme. The factors influencing the removal of BPA were also investigated. When the molar ratio of H_2O_2 and BPA was 1.5, the maximum removal effect could be achieved within 3 hours, pH had little influence on the removal rate of BPA, and 25℃ was the optimal temperature for the degradation reaction. The Michaelis-Menten kinetics showed that the affinity between enzyme and substrate decreased after immobilization. MIL-88B (Fe)/HRP has better thermal stability, storage stability and reusability than free HRP, which provides a possibility in industrial application.

Declarations

Acknowledgments:

This work was financed by introduced innovative R&D team leadership of Dongguan city (No. 2020607263005); National Natural Science Foundation of China (Project Approval No.: 21976060).

References

1. Besharati Vineh M, Saboury AA, Poostchi AA, Rashidi AM, Parivar K (2018): Stability and activity improvement of horseradish peroxidase by covalent immobilization on functionalized reduced graphene oxide and biodegradation of high phenol concentration. Int J Biol Macromol 106, 1314-1322
2. Bhatnagar A, Anastopoulos I (2017): Adsorptive removal of bisphenol A (BPA) from aqueous solution: A review. Chemosphere 168, 885-902
3. Bilal M, Barcelo D, Iqbal HMN (2020): Persistence, ecological risks, and oxidoreductases-assisted biocatalytic removal of triclosan from the aquatic environment. Sci Total Environ 735, 139194
4. Cao W, Yuan Y, Yang C, Wu S, Cheng J (2020): In-situ fabrication of g-C3N4/MIL-68(In)-NH2 heterojunction composites with enhanced visible-light photocatalytic activity for degradation of

ibuprofen. Chemical Engineering Journal 391

5. Chang Q, Tang H (2014): Immobilization of horseradish peroxidase on NH2-modified magnetic Fe3O4/SiO2 particles and its application in removal of 2,4-dichlorophenol. Molecules 19, 15768-82
6. Chang Q, Jiang G, Tang H, Li N, Huang J, Wu L (2015): Enzymatic removal of chlorophenols using horseradish peroxidase immobilized on superparamagnetic Fe3O4/graphene oxide nanocomposite. Chinese Journal of Catalysis 36, 961-968
7. Chang Q, Huang J, Ding Y, Tang H (2016): Catalytic Oxidation of Phenol and 2,4-Dichlorophenol by Using Horseradish Peroxidase Immobilized on Graphene Oxide/Fe(3)O(4). Molecules 21
8. Cheng J, Ming Yu S, Zuo P (2006): Horseradish peroxidase immobilized on aluminium-pillared inter-layered clay for the catalytic oxidation of phenolic wastewater. Water Res 40, 283-90
9. Dalal S, Gupta MN (2007): Treatment of phenolic wastewater by horseradish peroxidase immobilized by bioaffinity layering. Chemosphere 67, 741-7
10. Doherty CM, Grenci G, Ricco R, Mardel JI, Reboul J, Furukawa S, Kitagawa S, Hill AJ, Falcaro P (2013): Combining UV lithography and an imprinting technique for patterning metal-organic frameworks. Adv Mater 25, 4701-5
11. Escalona I, de Grooth J, Font J, Nijmeijer K (2014): Removal of BPA by enzyme polymerization using NF membranes. Journal of Membrane Science 468, 192-201
12. Gao C, Chen S, Quan X, Yu H, Zhang Y (2017): Enhanced Fenton-like catalysis by iron-based metal organic frameworks for degradation of organic pollutants. Journal of Catalysis 356, 125-132
13. Hong-Mei L, Nicell JA (2008): Biocatalytic oxidation of bisphenol A in a reverse micelle system using horseradish peroxidase. Bioresour Technol 99, 4428-37
14. Hou J, Dong G, Luu B, Sengpiel RG, Ye Y, Wessling M, Chen V (2014a): Hybrid membrane with TiO2 based bio-catalytic nanoparticle suspension system for the degradation of bisphenol-A. Bioresour Technol 169, 475-483
15. Hou J, Dong G, Ye Y, Chen V (2014b): Enzymatic degradation of bisphenol-A with immobilized laccase on TiO2 sol–gel coated PVDF membrane. Journal of Membrane Science 469, 19-30
16. Hu Y, Dai L, Liu D, Du W, Wang Y (2018): Progress & prospect of metal-organic frameworks (MOFs) for enzyme immobilization (enzyme/MOFs). Renewable and Sustainable Energy Reviews 91, 793-801
17. Jia Y, Chen Y, Luo J, Hu Y (2019): Immobilization of laccase onto meso-MIL-53(Al) via physical adsorption for the catalytic conversion of triclosan. Ecotoxicol Environ Saf 184, 109670
18. Laurier KG, Vermoortele F, Ameloot R, De Vos DE, Hofkens J, Roeffaers MB (2013): Iron(III)-based metal-organic frameworks as visible light photocatalysts. J Am Chem Soc 135, 14488-91
19. Lei ZD, Xue YC, Chen WQ, Li L, Qiu WH, Zhang Y, Tang L (2018): The Influence of Carbon Nitride Nanosheets Doping on the Crystalline Formation of MIL-88B(Fe) and the Photocatalytic Activities. Small 14, e1802045

20. Lin J, Liu Y, Chen S, Le X, Zhou X, Zhao Z, Ou Y, Yang J (2016): Reversible immobilization of laccase onto metal-ion-chelated magnetic microspheres for bisphenol A removal. Int J Biol Macromol 84, 189-99
21. Lin J, Hu Y, Wang L, Liang D, Ruan X, Shao S (2020): M88/PS/Vis system for degradation of bisphenol A: Environmental factors, degradation pathways, and toxicity evaluation. Chemical Engineering Journal 382
22. Lu Y-M, Yang Q-Y, Wang L-M, Zhang M-Z, Guo W-Q, Cai Z-N, Wang D-D, Yang W-W, Chen Y (2017): Enhanced Activity of Immobilized Horseradish Peroxidase by Carbon Nanospheres for Phenols Removal. CLEAN - Soil, Air, Water 45
23. Luo Z, Chen H, Wu S, Yang C, Cheng J (2019): Enhanced removal of bisphenol A from aqueous solution by aluminum-based MOF/sodium alginate-chitosan composite beads. Chemosphere 237, 124493
24. Pylypchuk IV, Daniel G, Kessler VG, Seisenbaeva GA (2020): Removal of Diclofenac, Paracetamol, and Carbamazepine from Model Aqueous Solutions by Magnetic Sol-Gel Encapsulated Horseradish Peroxidase and Lignin Peroxidase Composites. Nanomaterials (Basel) 10
25. Samui A, Sahu SK (2018): One-pot synthesis of microporous nanoscale metal organic frameworks conjugated with laccase as a promising biocatalyst. New Journal of Chemistry 42, 4192-4200
26. Shakerian F, Zhao J, Li SP (2020): Recent development in the application of immobilized oxidative enzymes for bioremediation of hazardous micropollutants - A review. Chemosphere 239, 124716
27. Shih Y-H, Lo S-H, Yang N-S, Singco B, Cheng Y-J, Wu C-Y, Chang IH, Huang H-Y, Lin C-H (2012): Trypsin-Immobilized Metal-Organic Framework as a Biocatalyst In Proteomics Analysis. ChemPlusChem 77, 982-986
28. Vineh MB, Saboury AA, Poostchi AA, Ghasemi A (2020): Biodegradation of phenol and dyes with horseradish peroxidase covalently immobilized on functionalized RGO-SiO2 nanocomposite. Int J Biol Macromol 164, 4403-4414
29. Vu TA, Le GH, Vu HT, Nguyen KT, Quan TTT, Nguyen QK, Tran HTK, Dang PT, Vu LD, Lee GD (2017): Highly photocatalytic activity of novel Fe-MIL-88B/GO nanocomposite in the degradation of reactive dye from aqueous solution. Materials Research Express 4
30. Wang S, Fang H, Wen Y, Cai M, Liu W, He S, Xu X (2015): Applications of HRP-immobilized catalytic beads to the removal of 2,4-dichlorophenol from wastewater. RSC Advances 5, 57286-57292
31. Wang X, Makal TA, Zhou H-C (2014): Protein Immobilization in Metal–Organic Frameworks by Covalent Binding. Australian Journal of Chemistry 67
32. Wu E, Li Y, Huang Q, Yang Z, Wei A, Hu Q (2019): Laccase immobilization on amino-functionalized magnetic metal organic framework for phenolic compound removal. Chemosphere 233, 327-335
33. Xiao F, Xiao P, Jiang W, Wang D (2020): Immobilization of horseradish peroxidase on Fe3O4 nanoparticles for enzymatic removal of endocrine disrupting chemicals. Environ Sci Pollut Res Int 27, 24357-24368

34. Xu J, Tang T, Zhang K, Ai S, Du H (2011): Electroenzymatic catalyzed oxidation of bisphenol-A using HRP immobilized on magnetic silk fibroin nanoparticles. Process Biochemistry 46, 1160-1165
35. Xu R, Chi C, Li F, Zhang B (2013): Immobilization of horseradish peroxidase on electrospun microfibrous membranes for biodegradation and adsorption of bisphenol A. Bioresour Technol 149, 111-6
36. Yi X, He X, Yin F, Yang T, Chen B, Li G (2020): NH2–MIL-88B–Fe for electrocatalytic N2 fixation to NH3 with high Faradaic efficiency under ambient conditions in neutral electrolyte. Journal of Materials Science 55, 12041-12052
37. Zdarta J, Antecka K, Frankowski R, Zgola-Grzeskowiak A, Ehrlich H, Jesionowski T (2018): The effect of operational parameters on the biodegradation of bisphenols by Trametes versicolor laccase immobilized on Hippospongia communis spongin scaffolds. Sci Total Environ 615, 784-795
38. Zhai R, Zhang B, Wan Y, Li C, Wang J, Liu J (2013): Chitosan–halloysite hybrid-nanotubes: Horseradish peroxidase immobilization and applications in phenol removal. Chemical Engineering Journal 214, 304-309
39. Zhang H, Wu J, Han J, Wang L, Zhang W, Dong H, Li C, Wang Y (2020a): Photocatalyst/enzyme heterojunction fabricated for high-efficiency photoenzyme synergic catalytic degrading Bisphenol A in water. Chemical Engineering Journal 385
40. Zhang L, Mi J, Hu G, Zhang C, Qi H (2020b): Facile fabrication of a high-efficient and biocompatibility biocatalyst for bisphenol A removal. Int J Biol Macromol 150, 948-954
41. Zhang R, Wang L, Han J, Wu J, Li C, Ni L, Wang Y (2020c): Improving laccase activity and stability by HKUST-1 with cofactor via one-pot encapsulation and its application for degradation of bisphenol A. J Hazard Mater 383, 121130

Figures

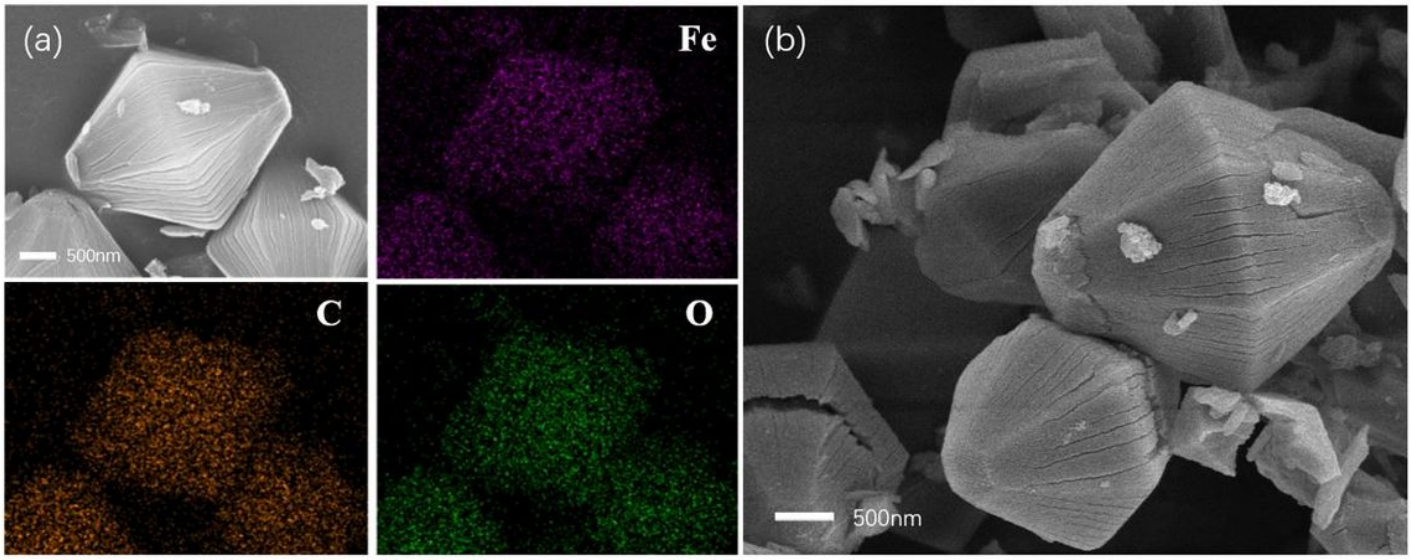

Figure 1

The SEM images of (a) MIL-88 (Fe), (b) MIL-88 (Fe)/HRP.

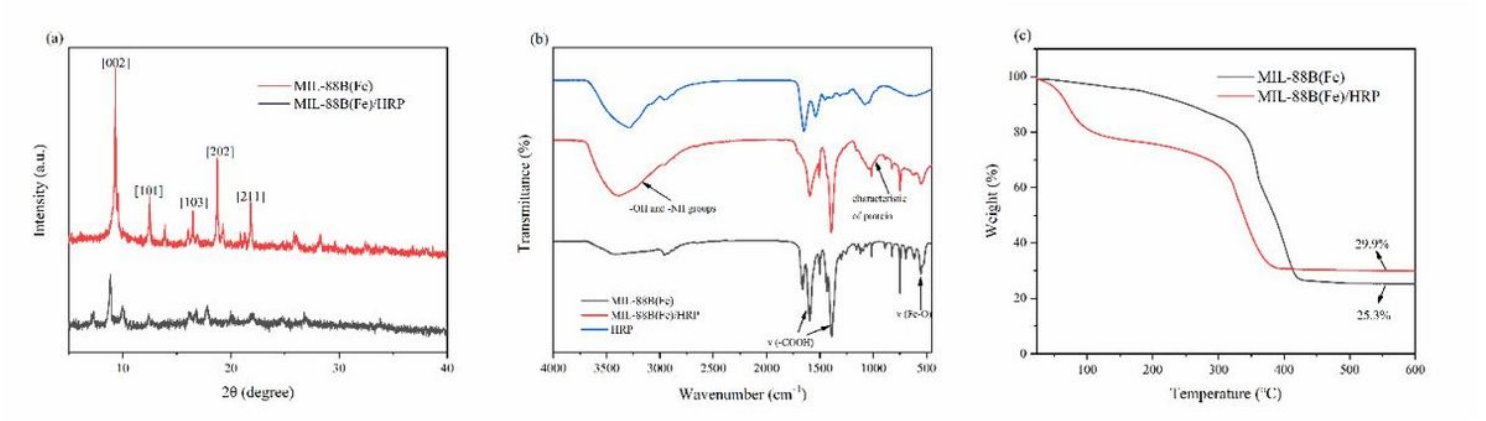

Figure 2

(a) XRD patterns, (b) FTIR spectra, (c) TG curves of MIL-88B(Fe) and MIL-88B(Fe)/HRP.

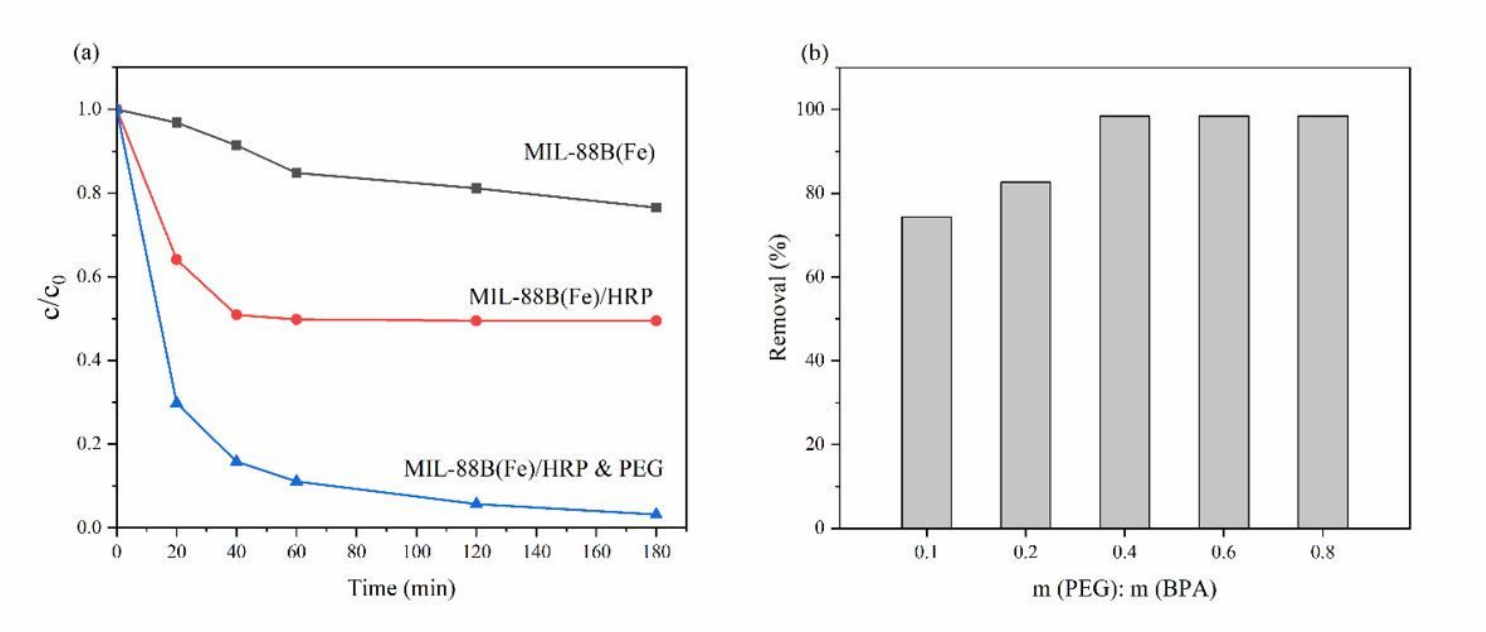

Figure 3

(a) Removal of BPA using different materials. (b) The effect of PEG dosage.

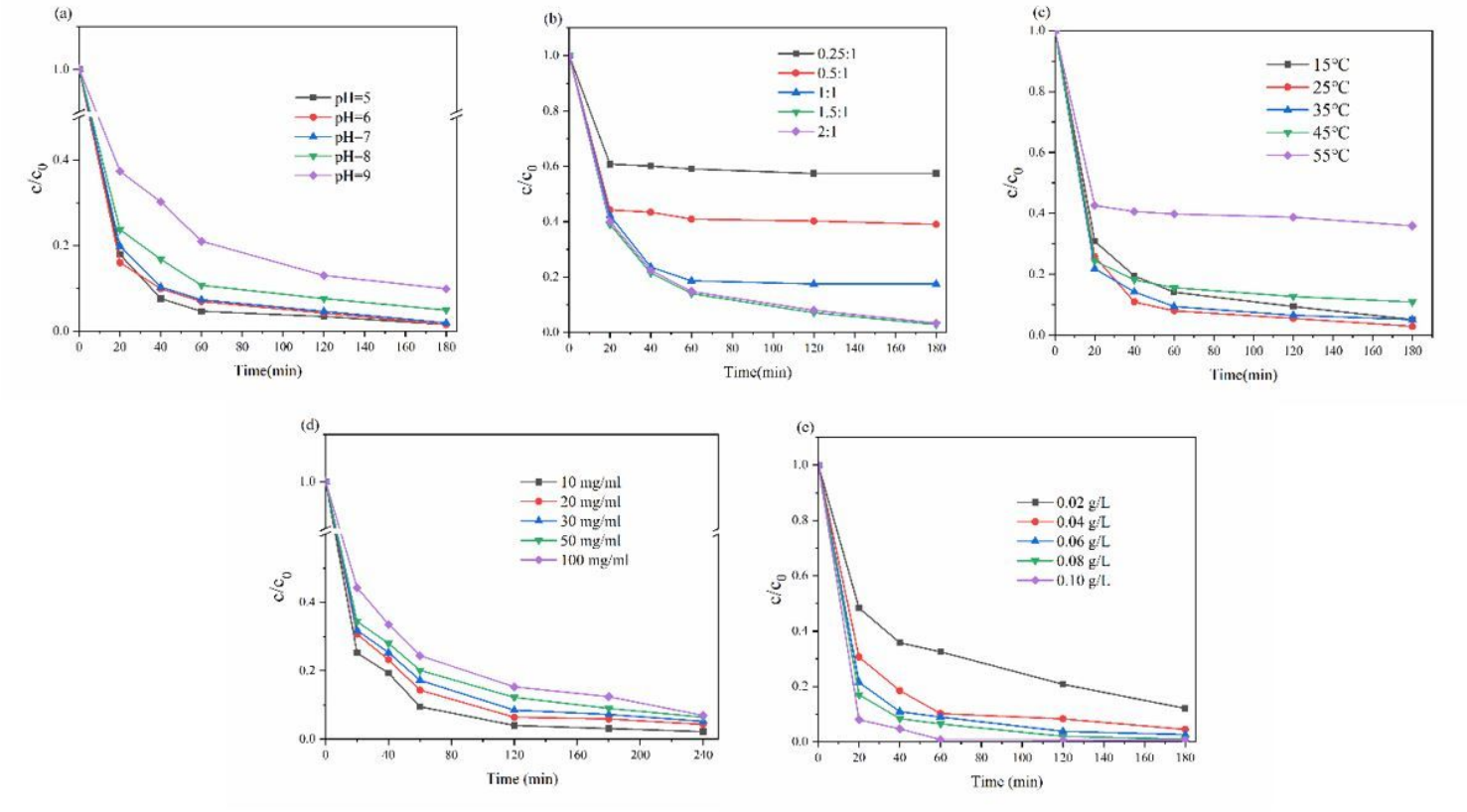

Figure 4

Effects of (a) pH, (b) H2O2 concentration, (c) reaction temperature, (d) BPA concentration, (e) catalyst dose on the degradation of BPA.

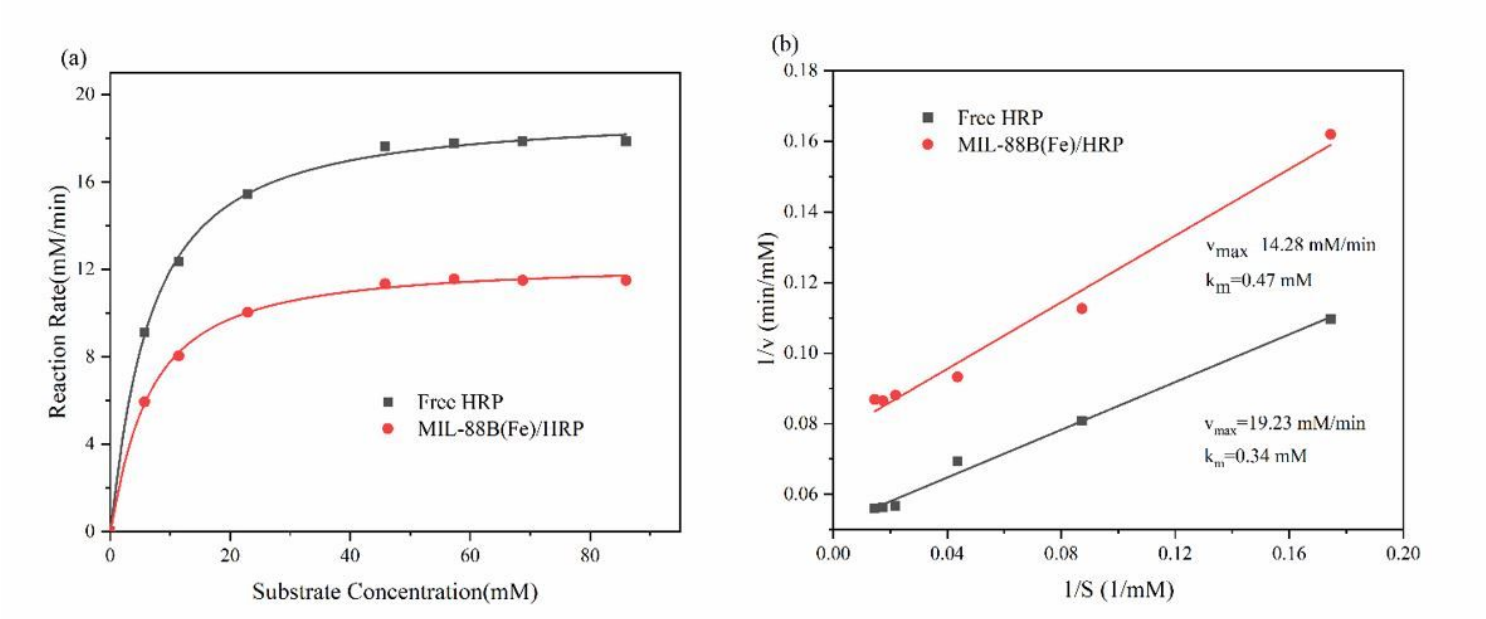

Figure 5

(a) Michaelis-Menten plots and (b) Lineweaver-Burk plots of free and immobilized HRP.

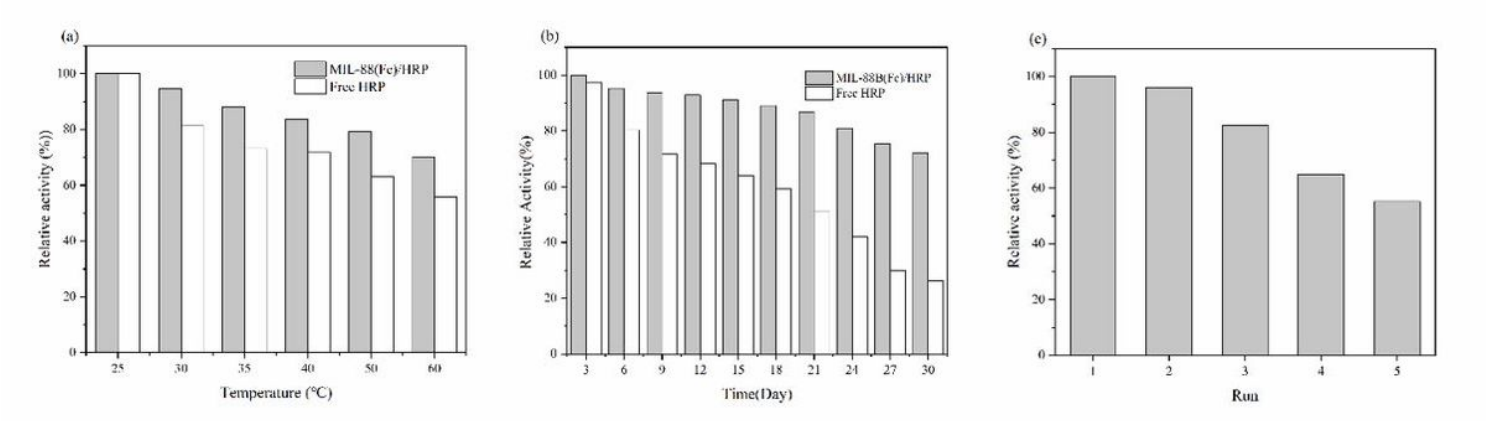

Figure 6

The stability of (a) temperature, (b) storage on free and immobilized HRP (c) reusability of immobilized HRP.